

1 **Effect of biopolymer matrices on lactose hydrolysis by enzymatically active hydrogel and**
2 **aerogels loaded with β -galactosidase nanoflowers**

3
4 María José Fabra^{1,2*}, David Talens-Perales³, Adrián Roman-Sarmiento³, Amparo López-Rubio^{1,2} and
5 Julio Polaina³

6
7 ¹ *Food Safety and Preservation Department Instituto de Agroquímica y Tecnología de Alimentos*
8 *(IATA-CSIC) Avda. Agustín Escardino 7, Paterna, Valencia, Spain.*

9 ² *Interdisciplinary Platform for Sustainable Plastics towards a Circular Economy- Spanish National*
10 *Research Council (SusPlast-CSIC), Madrid, Spain*

11
12 ³ *Biotechnology Department Instituto de Agroquímica y Tecnología de Alimentos, CSIC, Valencia,*
13 *Spain*

14
15
16 *Corresponding author.
17 *E-mail address: mjfabra@iata.csic.es*

18
19
20
21
22
23
24
25 _____

27 A B S T R A C T

28 In this work, enzymatically active polysaccharide-based hydrogels and aerogels have been developed.
29 To this end, a thermostable β -galactosidase (TmLac) enzyme from *Thermotoga maritima* embedded
30 in nanoflowers' format was used to evaluate the capacity of the hydrogel matrices to preserve the
31 hydrolytic activity of the enzyme and the reusability of the hydrogels formed. Commercial agar,
32 unpurified agar and agarose were compared as supporting materials. Although the developed hydrogel
33 capsules can be used at high temperature (75 °C) and reused for the digestion of lactose to a greater
34 extent than the free nanoflowers, loaded hydrogel capsules behaved differently depending on the type
35 of polysaccharide used. Commercial agar was the most promising one since these hydrogel capsules
36 could be reused, maintaining the structural integrity and reaching higher enzymatic activity (after
37 seven cycles at 75 °C) than the free TmLac-Ca²⁺ nanoflowers.

38 To facilitate handling and storage, aerogels were developed by freeze-drying the hydrogel capsules.
39 Aerogels of agarose and unpurified agar underwent structural changes during freeze-drying that
40 adversely affected their subsequent use, losing their integrity after being rehydrated. However,
41 commercial agar aerogels were successfully developed and reused thanks to the existing interactions
42 with TmLac-Ca²⁺ nanoflowers (confirmed by FTIR), which resulted in better capsule integrity and
43 enzyme protection. The hydrolytic activity of enzymatically active aerogels based on commercial agar
44 was in the same range of the free TmLac and TmLac-Ca²⁺ nanoflowers, being significantly higher to
45 their counterparts in the hydrated form (hydrogels based on commercial agar).

46 _____

47

48 *Keywords:*

49 β -galactosidase – hydrogel capsules -agar - milk products-nanoflowers-aerogels

50

51 _____

52 **1. Introduction**

53 Nowadays, about 75% of the world's adult population is lactose-intolerant (Silanikove, Leitner &
54 Merin, 2015) and people who suffer from lactose intolerance often reduce consumption of bovine
55 milk and other dairy products, which contain high quality proteins.

56 To overcome these issues, the food industry offers a wide range of lactose-free dairy products,
57 where lactose has been hydrolyzed into glucose and galactose so that also lactose intolerant
58 consumers can enjoy the variety of dairy products in their daily diet. The process of obtaining
59 these lactose-free products at industrial level consists of the direct addition of the fungal enzyme
60 β -galactosidase, generally obtained from *Kluyveromyces lactis* (Zolnere & Ciprova, 2018;
61 Dekker, Koenders & Bruins, 2019). However, this procedure has a disadvantage since the enzyme
62 remains in the final product (Chen et al., 2008) and is not being able to be reused. A very plausible
63 alternative is to immobilize the enzymes (Liese & Hilterhaus, 2013) which can result in increased
64 shelf-life and stability, allowing their recovery and reuse, thus having a positive impact on
65 production costs.

66 Furthermore, it is worth mentioning that, in order to reduce the risk of microbial contamination,
67 β -galactosidase enzymes coming from thermophilic microorganism are particularly attractive
68 because they can be easily purified by heat treatments (Marín-Navarro, Talens-Perales, Oude-
69 Vrielink, Cañada, & Polaina, 2014). This explains why, in the last decade, there has been an
70 increased interest in finding microorganisms and enzymes that meet these characteristics. In this
71 regard, *Thermotoga maritima* is a thermophilic bacterium with an optimal growth temperature
72 close to 80 °C (Huber et al., 1986) is a convenient source for heat-resistant enzymes like β -
73 galactosidase (TmLac) (Kim, Ji, & Oh et al. 2004).

74 The three-dimensional structure of TmLac has been recently reported by Minguez et al., 2020.
75 Furthermore, its immobilization by using different methodologies and supporting materials has
76 been also reported (Estevinho et al., 2018, Fabra et al., 2019). However, either costs or difficulties

77 in scaling-up immobilization technologies have mainly hampered industrial implementation
78 (Grosová, Rosenberg, & Rebroš, 2008).

79 In recent years, the use of micro- and nanomaterials for enzyme immobilization is gaining attention
80 because they have resulted in improved thermal stability and activity of the immobilized enzymes and
81 can also expand their applicability, and provide manipulation platforms to facilitate their use in
82 different field applications (Ansari & Husain, 2012, Hasanzadeh, Shadjou & de la Guardia., 2018,
83 Hong, Liu, Li, & Chen, 2019, Wang, Mohanty, & Mohanty, 2019). An interesting group of
84 nanomaterials is the so-called nanoflowers (Ge, Lei & Zare, 2012). Since its discovery, different
85 enzymes and other biomolecules have been immobilized with this technique (Liu et al., 2019). In this
86 regard, Talens-Perales, Fabra, Martínez-Argente, Martín-Navarro, & Polaina (2020) have recently
87 compared the efficiency of the immobilization of TmLac in the form of nanoflowers, using different
88 salts of Cu^{2+} , Mn^{2+} , Zn^{2+} , Co^{2+} and Ca^{2+} as inorganic compounds and being TmLac- Ca^{2+} nanoflowers
89 the most promising ones.

90 Even though nanotechnology has opened up a new frontier in the development of organic supports for
91 enzyme immobilization having positive results, one of the concerns is the application at large scale.
92 Furthermore, the separation process of these nanoflowers from the reaction medium at the end of the
93 catalytic process may be difficult and sometimes expensive, thus decreasing applicability (Cipolatti et
94 al., 2016, Cui & Jia, 2017). For this reason, combining physical adsorption of enzymes to
95 nanoflowers with encapsulation of these enzyme-containing nanoflowers within biopolymers can
96 be a good approach to solve some of the previously mentioned issues (Zhao et al., 2017, Bilal &
97 Iqbal, 2019).

98 Among biopolymers, agar is highly attractive for thermostable enzymes since upon solubilization in
99 hot water ($\sim 90\text{ }^\circ\text{C}$) and, under specific conditions, agar forms a slightly viscous fluid that can form
100 thermoreversible hydrogels when the temperature is decreased below a certain temperature (i.e.
101 gelling temperature). Agar is a hydrophilic linear polysaccharide derived from red seaweed (*Gelidium*,

102 *Pterocladia*, and *Gracilaria*) and contains alternating β -(1,3)- and α -(1,4)-linked galactose residues
103 with sulphated functional groups (Shankar & Rhim, 2017). It consists of a mixture of agarose and
104 agaropectin. Specifically, agarose is a linear polymer made up of repeating agarobiose units of
105 agarobiose, which is a disaccharide made up of D-galactose and 3,6-anhydro-L-galactopyranose and
106 it is the gelling component of agar. Many factors, such as the agar concentration, the amount and type
107 of impurities and the cooling rate affect the gelation mechanism of agar (Aymard et al., 2001, Lai &
108 Lii, 1997, Lee et al., 2017). At industrial scale, agar extraction process involves the application of
109 alkaline pre-treatments, which is critical for obtaining good quality agar although this treatment
110 significantly decreases the agar extraction yield. In contrast, unpurified agar (without alkali pre-
111 treatment) can be obtained using simpler procedures and with greater yields and the extracts contain
112 bioactive compounds such as proteins and polyphenols. These carbohydrates were selected as an
113 alternative to the widely used alginate for the formation of hydrogel capsules, since they can be
114 manipulated at the optimum temperature of TmLac (~ 75 °C) in gel form without being melted. The
115 preliminary hypothesis is that the gel strength, influenced by the inner structure of the hydrogel, will
116 be different depending on the material used (Martínez-Sanz et al., 2019) and will probably affect the
117 diffusion of the substrate (lactose) throughout the biopolymer network, thus resulting in different
118 lactose hydrolysis rates and degrees. The physical state of the supporting materials is supposed to also
119 affect the diffusion of substrate. Thus, hydrogel capsules (in which the dispersed phase within the
120 crosslinked biopolymer network is water) and aerogels (a more porous structure in which the water
121 has been replaced by air) will provide different enzymatic activity.

122 Considering these aspects, this work was designed to i) encapsulate TmLac- Ca^{2+} nanoflowers in
123 hydrogel structures based on seaweed-derived hydrocolloids in order to improve their handling
124 properties; ii) to evaluate commercial agar, unpurified agar and agarose (the gelling component of
125 agar) as encapsulation matrices in terms of lactose hydrolyzing capacity of the structures developed
126 thereof; and iii) to evaluate the physical state (hydrogel vs. aerogel) of the polysaccharide

127 encapsulating matrices on the enzymatic activity. Hydrogel capsules were prepared by means of a
128 novel methodology named “oil-induced biphasic hydrogel particle formation” previously described by
129 Alehosseini et al., 2019.

130

131 **2. Materials and methods**

132

133 *2.1. Chemical and reagents*

134 Salts used for nanoflowers formation (CaCl_2) or for buffer preparation (NaCl and MgCl_2), p-
135 nitrophenyl β -D-Galactopyranoside (pNP-Gal) and the glucose assay kit were purchased from
136 Sigma Aldrich. Lactose 1-hydrate was supplied by Panreac Quimica (Spain). Commercial agar,
137 the raw seaweed material (*Gelidium sesquipedale*) and agarose used as encapsulating matrices
138 were kindly donated by Hispanagar S.A. (Burgos, Spain). BlueSafe stain was supplied by
139 Nzytech. Sunflower oil was purchased from a local supermarket.

140

141 *2.2 Production and purification of TmLac*

142 Procedures used for the production and purification of TmLac from *Thermotoga maritima* are
143 described in Marin-Navarro et al. (2014). Briefly, cultures of *E. coli* Rosetta 2 strain, carrying
144 plasmid pQE-80L in which the TmLac encoding gene had been cloned, were induced to allow the
145 synthesis of histidine-tagged TmLac. The enzyme was purified from crude cell extracts in two
146 stages, first by thermal treatment at 85 °C, and then by nickel affinity chromatography.

147

148 *2.3 Production of TmLac-inorganic nanoflowers*

149 Nanoflowers were obtained by the procedure described by Ge et al. (2012) with some
150 modifications as described by Talens-Perales et al (2020). Briefly, a stock solution of TmLac was
151 firstly prepared in phosphate-buffered saline (PBS) at a final concentration of 0.05 mg/mL and,

152 then, 20 μL of 120 mM CaCl_2 solution were added to 1500 μL of the enzyme solution and
153 incubated at room temperature (23 ± 2 °C) for 24 h. After this time, nanoflowers, which appeared
154 as a precipitate sediment, were washed with PBS and resuspended in assay buffer (50 mM
155 phosphate buffer, pH 6.5, 10 mM NaCl, 1 mM MgCl_2). The presence and activity of TmLac in
156 the nanoflowers was tested enzymatically by the remaining activity in the supernatant after
157 nanoflower formation, by using 5 mM *p*-nitro phenyl β -D-galactopyranoside (pNP-Gal) as the
158 substrate (Talens-Perales et al., 2020).

159

160 2.4. Preparation of hydrogel capsules and aerogels

161 Hydrogel capsules containing TmLac- Ca^{2+} nanoflowers was performed following a protocol
162 adapted from Alehosseini *et al.*, 2019. In brief, an aliquot of 200 μL of nanoflowers resuspended
163 in buffer were mixed with 200 μL stock polysaccharide aqueous solutions (commercial agar,
164 unpurified agar and agarose) (see Supplementary material S1). Stock polysaccharide aqueous
165 solutions were previously prepared by dissolving the required amount of each polysaccharide in
166 hot water at ~ 90 °C to have a final concentration of 1% (w/v) of commercial agar or agarose and
167 3.5 % (w/v) of unpurified agar. Then, solutions were cooled until approx. 40 °C and introduced
168 in a 5 mL plastic syringe with a yellow pipette tip. Hydrogel capsules were formed by dripping
169 the nanoflowers-containing polysaccharide based solutions into a biphasic bath containing an
170 upper sunflower oil layer and a lower cold water layer, for the collection of the hydrogel particles.
171 Control hydrogel capsules (without nanoflowers) were prepared for comparative purposes.

172 Aerogels, with and without nanoflowers, were prepared by freeze-drying the hydrogel capsules
173 using a Genesis 35-EL freeze-dryer (Virtis). To this end, hydrogel samples were frozen in liquid
174 nitrogen ($T \leq -210$ °C) and kept in a freezer at -80 °C until being lyophilized.

175 Unpurified agar, used as encapsulating matrix, was previously obtained following the procedure
176 described by Martínez-Sanz et al., 2019. Briefly, 50g of seaweed powder were immersed in 500

177 mL of distilled water and heated up to 90 °C for 2h. The agar-based solution was subsequently
178 separated from the solid residue by filtration with a muslin cloth and the filtrate was allowed to
179 gel and then, it was frozen overnight at - 21 °C. Afterwards, the material was subjected to two
180 freeze-thaw cycles (-21 °C/25°C) to improve the elastic properties of the gels and the obtained
181 material was freeze-dried for further use. The unpurified agar extract was characterized, having
182 392 ± 77 mg/g of carbohydrates (~ 75% galactose), 136 ± 9 mg BSA/g of proteins and 30 ± 2 mg
183 GA/g of polyphenols and 2.8 ± 0.2 % of sulphates (Martínez-Sanz et al., 2019). This explains the
184 higher concentration needed to form gels from the unpurified agar used as encapsulation matrix
185 when compared to that from commercial agar and agarose.

186

187 *2.5. Scanning Electron Microscopy (SEM)*

188 Aerogels were observed in a Hitachi SEM microscope (Hitachi S-4800) at an accelerating
189 voltage of 10 kV and a working distance of 8.0 – 8.5 mm. Samples were mounted on an
190 Aluminium Specimen Mounts, fixed on the support using double-side adhesive tape and coated
191 with a thin layer of gold-palladium sprayed on their surface. Cross-section of aerogels were
192 explored by cryo-fracturing them after immersion in liquid nitrogen, before being mounted on the
193 aluminum support.

194

195 *2.6. Enzymatic activity assays*

196 Enzyme activity determinations were carried out, in triplicate, at the optimum pH (6.5)
197 and temperature (75 °C) of the enzyme, using lactose as the substrate. Nanoflowers, free or
198 encapsulated, were washed with PBS at room temperature to remove residual unbound enzyme
199 and dispersed in 5% (w/v) lactose in the assay buffer for 30 min. Reactions were finished by
200 heating at 95 °C for 10 minutes. Lactase activity was measured by quantifying the amount of
201 glucose released, using a glucose assay kit (Sigma).

202 In order to obtain the kinetics of lactose hydrolysis, the incubations were performed at 75
203 °C for 8 h in 5% (w/v) lactose in assay buffer, taking an aliquot after the first 30 min and, then,
204 after every hour. Lactose hydrolysis at each incubation time was measured as already explained.

205 The possibility of reusing the hydrogel and aerogels capsules was tested by subjecting
206 them to consecutive cycles of lactose hydrolysis at 75 °C for 3.5 h with gentle agitation. After each
207 incubation time, samples were recovered by centrifugation and washed with assay buffer before being
208 placed again with assay buffer with 5% (w/v) lactose for the following reaction cycle. Remaining
209 lactose in the supernatant of the reaction, after each cycle, was estimated as a function of the amount
210 of glucose measured with a Glucose (GO) Assay Kit.

211

212 *2.7. Color analysis of immobilized nanoflowers labelled with BlueSafe*

213 To visually observe the immobilized nanoflowers within the hydrogel capsules, capsules
214 were stained with a protein stain called BlueSafe. To this end, loaded and unloaded hydrogel
215 capsules were stained with BlueSafe during 2h and then, capsules were washed overnight with
216 distilled water to remove residual stain. Finally, samples were observed by means of a digital
217 microscope EVO CamII (Vision Engineering, United States).

218

219 *2.8. Fourier transform infrared (FT-IR) analysis of the materials*

220 The attenuated total reflectance (ATR)-FTIR spectra of the freeze-dried capsules were obtained
221 in a Thermo Nicolet Nexus equipment. The acquisition time was 128 s at 4 cm⁻¹ resolution, and
222 the average spectra in the 4000-400 cm⁻¹ range are reported.

223

224 *2.9. Gel strength*

225 The gel strength was measured by using a TA-XTplus Texture Analyser (Stable Micro Systems,
226 Surrey, UK), with a 5 N load cell, using a 2mm diameter cylindrical probe. Hydrogel capsules

227 were 50% compressed at 1 mm/s deformation rate. Measurements were carried out in ten hydrogel
228 capsules.

229 230 2.10 Statistical analysis

231 Statistical analysis of experimental data was carried out with the IBM SPSS Statistics
232 software (v.23) (IBM Corp., USA) through the analysis of variance (ANOVA). Comparison of
233 the means was done using the Tukey's Honestly Significant Difference (HSD) at 99% confidence
234 level.

235

236 3. Results and discussion

237

238 3.1 Enzymatically active hydrogel capsules based on commercial agar, unpurified agar and 239 agarose.

240 Figure 1 shows representative images of the polysaccharide hydrogel capsules prepared with and
241 without TmLac-Ca²⁺ nanoflowers. As clearly observed, all capsules were similar in shape and
242 size (~2 mm diameter), being apparently rougher those prepared with unpurified agar. In order to
243 qualitatively evaluate the presence and distribution of nanoflowers in the loaded capsules, the
244 protein (TmLac) was stained with BlueSafe, which is a highly sensitive single step protein-
245 specific stain. As expected, unloaded agarose hydrogel capsules (without TmLac-Ca²⁺
246 nanoflowers) were not stained. However, a bluish coloration was observed in commercial agar-
247 based hydrogel capsules, which is indicative of the presence of proteins deriving from the native
248 algae, which had not been eliminated during the extraction process. In fact, it is worth mentioning
249 that *Gelidium sesquipedale* has about 30% protein (Faraj, Lebbar, Debry & Najim, 1987) and,
250 thus, it is possible that a small amount of proteins remained after the industrial purification
251 process with sodium hydroxide, which is performed prior to the agar extraction. In fact, a more
252 intense blue color was observed for the hydrogels prepared from unpurified agar, in agreement

253 with the compositional analysis results of these extracts (136 mg BSA/g of proteins, Martínez-
254 Sanz et al., 2019) and as it was also evidenced by FTIR analysis (as shown below).

255 The incorporation of enzyme-loaded nanoflowers caused a significant increase in the intensity of
256 bluish coloration, which was closely related to the presence of the TmLac and a homogeneous
257 distribution of blue color was observed throughout the hydrogel capsules indicating that
258 nanoflowers were well-distributed within the hydrocolloid matrices. Differences in the bluish hue
259 of loaded hydrogel capsules evidenced a synergetic effect between proteins remaining in the agar
260 matrices and TmLac-Ca²⁺ nanoflowers. Accordingly, the intensity of the bluish coloration in
261 agarose-loaded samples was significantly lower due to the absence of proteins in the unloaded
262 pure agarose matrix (Figure 1E), indicating that the blue color in loaded agarose samples only
263 corresponded to the contribution of TmLac-containing nanoflowers.

264 The enzymatic activity of the immobilized enzyme was assessed by incubating hydrogel capsules
265 in lactose 5% (w/v). For comparative purposes, the free enzyme and TmLac-Ca²⁺ nanoflowers
266 were also incubated at an equivalent concentration. It should be highlighted that direct
267 incorporation of the TmLac within the three hydrogel matrices was also attempted for comparison
268 purposes, but it resulted in leaking of the enzymes to the media and, thus, no remaining
269 hydrolyzing activity of the hydrogel capsules produced, thus requiring the pre-immobilization
270 step in nanoflowers to deliver enzymatically active materials. Table 1 shows the specific activity
271 (measured after 30 min of incubation with lactose) and Figure 2 gathers the kinetics of lactose
272 hydrolysis of the free TmLac, TmLac-Ca²⁺ nanoflowers and hydrogel capsules loaded with
273 TmLac-Ca²⁺ nanoflowers. As observed, TmLac-Ca²⁺ nanoflowers behaved similarly to the free
274 enzyme, in agreement with the results recently reported by Talens-Perales et al., (2020). However,
275 a significant decrease ($p < 0.05$) in the enzymatic activity was observed in the loaded hydrogel
276 capsules.

277 As expected, the immobilized enzyme was slightly less efficient than the unprotected TmLac-
278 Ca²⁺ nanoflowers in the conditions tested (Fig. 2), reaching around 85 % hydrolysis after about 3
279 h of incubation with lactose. Similarly, Panesar, Kumari, & Panesar 2011 reported 85% of lactose
280 hydrolysis of enzymatically active permeabilized *Kluyveromyces marxianus* cells immobilized
281 into alginate hydrogels and incubated during two hours. Although the differences were small, the
282 presence of impurities interacting with the agar seemed to affect the specific hydrolytic activity
283 of the encapsulated TmLac-Ca²⁺ nanoflowers. This seems to be related to two different factors:
284 (i) the diffusion of substrate through biopolymer matrices, which may be restricted in hydrated
285 systems (hydrogels) and (ii) the biopolymer gel network structure, which will impact the strength
286 of the hydrogel capsules. The catalytic activity of the immobilized enzymes is greatly affected by
287 the porosity, particle size and polarity of the hydrogel matrix, amongst others, as all these factors
288 have an impact on diffusion kinetics (Drozdov, Papadimitriou, Liely & Sanporean, 2016; Nieto
289 et al., 2010) and, thus, the gel structure was expected to affect enzyme accessibility and,
290 consequently, result in slightly decreased enzymatic activity, when compared to that displayed
291 by free enzymes. Additionally, the inherent highly hydrated state of the hydrogel capsules also
292 poses additional substrate (lactose) diffusion restrictions for accessing the active enzyme sites, as
293 water is strongly bonded to form a three-dimensional polymeric network providing mechanical
294 integrity and flow resistance.

295 To confirm this hypothesis, the mechanical properties of the hydrogel capsules were evaluated by
296 means of penetration tests. Table 2 summarizes the calculated gel fracture strength values for the
297 loaded and unloaded hydrogel capsules. The first thing to highlight is that hydrogel capsules
298 prepared with unpurified agar could not be measured. This can be ascribed to the presence of
299 unpurified compounds (polyphenols, proteins) which greatly affect the gel strength. This
300 hypothesis was reinforced by comparing the agarose capsules with and without nanoflowers, since
301 the incorporation of nanoflowers negatively affected the gel strength presumably because the

302 presence of nanoflowers could impair the hydrogen-bonding network formation, thus affecting
303 the resulting microstructure. Agar hydrogel capsules are an intermediate between a solid and
304 liquid having both elastic (solid) and flow (liquid) characteristics. The agar gelation process has
305 been widely reported in literature (Guenet & Rochas, 2006, Matsuo, Tanaka, & Ma, 2002,
306 Stanley, 2006). The microstructure of agar hydrogels revealed a porous network made of bundles
307 of agarose helices (Chui, Phillips & McCarthy, 1995, Nordqvist & Vilgis, 2011), in which the
308 agaropectin do not participate in the gel network and obstruct the pores. Thus, TmLac-Ca²⁺
309 nanoflowers would affect the gelation mechanism of agarose since it would interfere in the
310 formation of hydrogen bonds between agarose chains (the gelation component of the agar). In
311 contrast, this effect was not observed in the commercial agar, where the presence of nanoflowers
312 did not cause significant changes in the gel strength of the hydrogel capsules ($p>0.05$), thus,
313 suggesting that the presence of agaropectin in the commercial agar samples was responsible of
314 this different behavior as it will be later on confirmed by FTIR analysis (see below). Furthermore,
315 these results are also in line with the enzymatic activity results, highlighting that, as suggested,
316 hydrogel network organization, resulting in different gel strength, has an impact on substrate
317 diffusion as, indeed, the loaded agar capsules with greater gel strength were the ones in which a
318 lower enzymatic activity was observed.

319 The recyclability of the immobilized enzyme after consecutive incubations with 5% (w/v) lactose
320 at 75 °C was also tested. As shown in Figure 3, the enzymatic activity of the nanoflowers
321 decreased about 65% after four incubation rounds and, a slighter but progressive decay of activity
322 was observed, albeit to a lesser extent, in subsequent incubations. Loaded capsules behaved
323 differently depending on the type of carbohydrate-based encapsulating matrix used. Interestingly,
324 a statistically significant increase in the hydrolysis activity after the first batch was observed in
325 hydrogel capsules formed either with commercial agar or with agarose. This increase was in
326 accordance with that reported for agarose-alginate hydrogel capsules in which bacterial cells

327 loaded with a TmLac were embedded (Fabra et al., 2019). This phenomenon suggests that, after
328 the first incubation at 75 °C, these hydrogel matrices underwent a structural change, promoting
329 the mobility of molecular chains and leading to the formation of less densely packed structures.
330 This structural relaxation phenomenon was the responsible of the better diffusion of lactose
331 (substrate) through the encapsulation matrix, as it was previously demonstrated for
332 alginate/agarose hydrogel capsules (Fabra et al., 2019). After the second incubation, a progressive
333 decay of activity (in both commercial agar and agarose) was observed, reaching a total loss of
334 ~50 % after seven hydrolysis batches. Nevertheless, the enzymatic activity of the agarose and
335 commercial agar hydrogel capsules was greater for each incubation cycle than for the free
336 nanoflowers, being this enhanced hydrolytic activity attributed to the enzyme protection effect of
337 the hydrogel matrices. Similarly, TmLac-immobilized on the surface of epoxy-coated magnetic
338 beads was able to hydrolyze more than 60 % of the lactose after eight incubations cycles (Marín-
339 Navarro et al., 2014).

340 In contrast, although the enzymatic activity obtained for hydrogel capsules made from unpurified
341 agar showed the same trend as those obtained with commercial agar and agarose, the lactose
342 hydrolysis after each incubation cycle was considerably lower ($p < 0.05$) than that of the loaded
343 commercial agar or agarose-based capsules and even from the activity obtained using the free
344 nanoflowers, reaching an enzymatic activity loss around 86%, which was similar to that obtained
345 for free nanoflowers, after the seven batches. As mentioned before, the presence of other
346 compounds (i.e. proteins, polyphenols) in the unpurified agar reduced the gelling capacity of the
347 agar since they interfered in the self-assembling of agarose molecules (via hydrogen bonding)
348 during the gelation process and thus, softer gels with less dense network were formed, as it has
349 been previously confirmed by the mechanical analysis. These less dense structures are
350 hypothesized to offer less protection to the loaded enzymes, thus resulting in similar performance
351 when compared with the TmLac-containing nanoflowers.

352

353 *3.2 Enzymatically-active aerogels based on agar.*

354 In an effort to increase the activity and stability of immobilized enzymes, aerogels were formed
355 by freeze-drying, aiming to increase their handling and applicability as compared to their
356 counterparts prepared in the hydrated form. Furthermore, the substrate (lactose) diffusion through
357 the biopolymer network is also expected to be improved due to the absence of water molecules
358 in the pristine aerogel network. In fact, it is expected that aerogels quickly absorb water by
359 capillarity and thus, the substrate once it will be in contact with the lactose solution. Aerogels are
360 solids that feature very low density, high specific surface area and consist of a coherent open-
361 porous network of loosely-packed chains which are formed by replacement of the liquid in a gel
362 with gas (Ubeyitogullari, Brahma, Rose & Ciftci, 2018). Thus, hydrogel capsules based on
363 commercial agar, unpurified agar and agarose were freeze-dried and the enzymatic activity of the
364 aerogel structures was tested. The visual appearance of the developed aerogels is shown in Figure
365 4, where it is evidenced that whereas those prepared with commercial agar and agarose presented
366 a whitish hue (being more opaque in the case of commercial agar), the aerogel prepared with
367 unpurified agar showed a brownish hue, mostly due to the presence of proteins and polyphenols.
368 The microstructure and porosity of the aerogels formed were also examined by scanning electron
369 microscopy (SEM). Figures 5 and 6 show the surface and cross-section images of the different
370 loaded and unloaded aerogels structures, respectively. Representative micrographs of a detail of
371 some nanoflowers on the surface of the hydrogel capsules covered by different biopolymer
372 matrices are also given in Figure 5. The estimated porous area, which has been obtained from the
373 binary images of SEM micrographs, is also given in Figure 6. As observed, agarose aerogels
374 showed a denser microstructure, in agreement with previous works using other biopolymers such
375 as κ -carrageenan and β -glucan to produce aerogels (Comin, Temelli, & Saldaña, 2012; Manzocco
376 et al., 2017). In contrast, agar-based aerogels showed a less compact network, being the pore size

377 of freeze-dried unpurified agar samples even higher than in the commercial agar aerogels (see
378 Figure 6), as expected from the presence of other components which could interfere in the gelation
379 process of the agarose (gelling component of the agar). Interestingly, the effect that the
380 nanoflowers had on the microstructure of the aerogels depended on the biopolymer used as
381 supporting material. It was clearly observed that nanoflowers were not properly integrated within
382 the agarose matrix (Figure 5C), being not accurately covered by the biopolymer and promoting
383 the formation of a less dense structure with higher pore size than its counterpart prepared without
384 nanoflowers. In contrast, a decrease in the average pore size (as well as in the porous area, see
385 Figure 6) was observed in agar-based aerogels incorporating nanoflowers, providing a denser
386 structure than their unloaded counterparts and being more marked in the case of commercial agar.
387 Therefore, it is reasonable to think that nanoflowers will be better protected by commercial agar-
388 based matrices and, thus, the enzymatic activity will be better preserved. These findings
389 evidenced potential interactions between the agaropectin (the non-gelling fraction of agar) and
390 TmLac-Ca²⁺ nanoflowers, as it will be later on confirmed by FTIR analysis (see below).
391 Agaropectin is a charged polysaccharide, composed of agarose and varying percentages of ester
392 sulphate, D-glucuronic acid and small amounts of pyruvic acid (Labropoulos, Niesz, Danforth, &
393 Kevrekidis, 2002), which interact with the calcium ions arriving from the CaCl₂ salt used for
394 nanoflowers' formation. However, these interactions could be limited in unpurified agar due to
395 the presence of other components.

396 It should be noted that, despite of being properly freeze-dried, neither the unpurified agar samples
397 nor the agarose samples could be used after freeze-drying since they disintegrated after a few
398 minutes of rehydration. This also suggests that some structural and molecular changes occurred
399 in the aerogels depending on the carbohydrate used as supporting material, as it was anticipated
400 by the SEM images and confirmed by FTIR (see below). In fact, similar effects were previously

401 reported for freeze-dried agarose microspheres (Nweke, Turmaine, McCartney, & Bracewell,
402 2017).

403 Thus, in order to further investigate potential molecular interactions between the processed
404 matrices, ATR-FTIR spectra of loaded and unloaded aerogels were recorded. As observed in
405 Figure 7, all the samples presented the most characteristic bands from agar, located at 1260 cm^{-1}
406 and 1371 cm^{-1} assigned to the presence of sulphate ester groups (Volery, Besson, & Schaffer-
407 Lequart, 2004) and at 1150 cm^{-1} ascribed to the vibration mode of ester-sulphate linkages of D-
408 galactose (Chopin, Kerin, & Mazerolle., 1999). The vibrational bands at 1030 and 930 cm^{-1}
409 correspond to the C-O stretching group of the 3, 6-anhydro-D-galactose, while the band at 890
410 cm^{-1} can be assigned to the C-H bending at the anomeric carbon in β -galactopyranosyl residues
411 (Gómez-Ordoñez & Rupérez, 2011, Shankar & Rhim, 2017). It is worth nothing that while the
412 commercial agar and agarose aerogels showed two bands located at 1360 cm^{-1} and 1430 cm^{-1} , the
413 aerogels based on unpurified agar presented a broader band centered at 1400 cm^{-1} . Furthermore,
414 although the amide I band, typically located at 1653 cm^{-1} was masked by the intensity of the band
415 characteristic of physisorbed water (centered at 1630 cm^{-1} approximately), the amide II band
416 (located at 1540 cm^{-1}) was observed in the unpurified agar, evidencing the presence of a
417 significant amount of proteins (as it has been demonstrated by the BlueSafe staining, see Figure
418 1). In fact, the higher intensity of these bands clearly evidenced the higher content of proteins in
419 unpurified agar when compared to that of commercial agar or agarose.

420 All aerogel samples prepared with agar or agarose showed bands in the range of 2840 - 2950 cm^{-1} ,
421 1 , ascribed to the symmetric and asymmetric vibrations of the alkane groups of the agar
422 biopolymer chain (Rhim, Wang, Lee, & Hong, 2014). Interestingly, it was observed that the
423 spectral band at 2936 cm^{-1} split in two when nanoflowers were incorporated into commercial agar
424 aerogels and, the band located at 1371 cm^{-1} , attributed to sulphate groups shifted toward higher
425 wavenumbers, suggesting that there were some interactions between the commercial agar and the

426 TmLac-Ca²⁺ nanoflowers. Specifically, the negative charge of sulphate groups from agaropectins and
427 the positive charge of calcium ions from the nanoflowers could interact, favoring the formation of
428 agaropectin complexes via sulfonate esters. As a result, these molecular interactions, probably fostered
429 by the dehydration process during freeze-drying, could explain the differences observed in aerogels'
430 microstructure (being denser in loaded agar-based aerogels) and their subsequent integrity during
431 enzymatic activity testing. Similarly, interactions between Ca²⁺ and the S=O stretching groups of the
432 sulphate ester groups from carrageenan have also been reported by Levy-Ontman et al., 2019.

433 The broad absorption band in the region of 2900 and 3800 cm⁻¹ corresponds to hydroxyl group
434 vibrational stretching and it is associated to OH bond in water or hydroxyl groups of the agarose,
435 and agar-based samples. Due to the hydrophilic nature of these samples, some water adsorption
436 occurred under environmental conditions and, this was also observed by the above-mentioned
437 bending vibration at 1640 cm⁻¹, characteristic of physisorbed water. As expected, the relative
438 intensity of these bands was higher for unpurified samples due to the presence of other hydrophilic
439 compounds in the matrix, which were not present in the commercial agar. Interestingly, a
440 reduction in the peak intensities of the previously mentioned vibrational bands was observed for
441 loaded commercial agar and unpurified agar-based samples but not in loaded agarose samples, as
442 compared to their unloaded counterparts. This suggests that hydrogen bonding interactions
443 between agaropectin (the non-gelling fraction of agar) and the nanoflowers took place, being
444 more evident in the case of commercial agar where the reduction of the bands' intensity was even
445 higher. As a consequence, these interactions favor the formation of a denser structure in aerogels
446 formed with commercial agar and, the higher porosity observed in unpurified agar and agarose
447 aerogels could be the responsible of the loss of their integrity after being rehydrated.

448 Therefore, taking into account these findings, the enzymatic activity and reusability of the aerogels
449 were carried out with commercial agar aerogels loaded with TmLac-Ca²⁺ nanoflowers. The effect of
450 the freeze-drying process on the specific enzymatic activity (measured after 30 min of incubation with

451 lactose) of the free enzyme (TmLac) and the corresponding nanoflowers were firstly evaluated and
452 compared with the agar-based aerogels (supplementary material S2). While no differences were
453 observed between fresh and freeze-dried free TmLac, combining nanoflowers with the freeze-drying
454 process resulted in a lower enzymatic activity (around ~ 52%) of the TmLac-Ca²⁺ nanoflowers, as
455 compared to their freshly-prepared counterparts. This can be ascribed to structural changes occurring
456 in nanoflowers during the dehydration process which could negatively affect the catalytic activity of
457 the enzyme. Interestingly, commercial agar aerogels showed a specific activity similar to the free
458 TmLac enzyme indicating that the agar matrix exerted a protective effect on the TmLac-Ca²⁺
459 nanoflowers likely attributed to the interactions with the encapsulating matrix, as previously observed
460 by FTIR. Besides, it is worth mentioning that the specific activity of the freeze-dried samples was
461 significantly higher ($p < 0.05$) than their counterparts in the hydrated form, reaching values in the range
462 of the free TmLac. This confirms that aerogels, structured dry materials with high porosity and large
463 surface area (as previously observed in Figure 6), allowed a faster penetration of the 5% (w/v) lactose
464 (substrate) aqueous solution, thus accelerating the hydrolytic activity.

465 Once the methodology was proved to successfully increase the hydrolytic activity of the enzymatically
466 active materials, the reaction kinetics of the commercial agar based aerogels was also explored. From
467 Figure 8, a similar pattern was observed between agar-based aerogels and free TmLac or freshly-
468 prepared TmLac-Ca²⁺ nanoflowers, reaching the plateau after 3.5 h incubation. Therefore, this time
469 was chosen to subject the samples to repeated batched of lactose hydrolysis. As shown in Figure 9,
470 agar-based aerogels behaved similar to the hydrated samples (see Figure 3), showing a progressive
471 decrease in the enzymatic activity after each cycle and, resulting in a ~ 33% of hydrolytic activity
472 decay after the third incubation round. Although the hydrated material allowed one more cycle of
473 reuse, reaching a decrease of ~27% in the fourth cycle (see Figure 3), enzymatically active
474 aerogels facilitate the handling and storage of the enzyme with respect to its hydrated
475 counterparts.

476

477 **4. Conclusion**

478 Three different seaweed-derived matrices (commercial agar, unpurified-agar and agarose) have been
479 used to produce enzymatically active hydrogels and aerogels containing TmLac-Ca²⁺ nanoflowers.
480 The results evidenced that the composition, which conditioned the gel strength of hydrogel capsules,
481 had a strong impact on the properties of the formed hydrogels and on its hydrolytic activity and
482 reusability for the digestion of lactose at high temperature (75 °C). Although hydrogel capsules
483 prepared with commercial agar were the best performing materials, which could be reused during
484 seven consecutive cycles at 75°C, keeping a higher enzymatic activity (after seven cycles at 75 °C)
485 than the non-encapsulated TmLac-Ca²⁺ nanoflowers, its freeze-dried counterpart (commercial agar
486 aerogel) improved handling and storage stability of the developed enzymatically active materials
487 without detrimentally affecting neither its hydrolytic activity nor its reusability at high temperatures.
488 From the results obtained, aerogels based on commercial agar displayed high catalytic activity (i.e. 0.5
489 g of aerogel capsules hydrolyzed the lactose equivalent of 100 mL of milk in 15 min) and thermal
490 stability.
491 These results add new insight, to other previous studies, into the potential of this processing method
492 for the development of enzymatically active materials of significant interest in the dairy industry with
493 the additional advantage that they can be easily scaled-up.

494

495 **Acknowledgment**

496 This research was supported by grants from Spain's 'Secretaría de Estado de Investigación, Desarrollo
497 e Innovación' (AGL2016-75245-R), Agencia Estatal de Investigación (AEI, Grant PCI2018-092886)
498 and cofunded by the European Union's Horizon 2020 research and innovation programme (ERA-Net
499 SUSFOOD2). MJF was supported by a Ramon y Cajal contract (RYC2014-15842) from the Spanish
500 Ministerio de Economía; Industria y Competitividad. The authors thank the Central Support Service

501 for Experimental Research (SCSIE) of the University of Valencia for the electronic microscopy
502 service.

503

504 **References**

505 Alehosseini, A., Gomez del Pulgar, E.-M., Fabra, M.J., Gómez-Mascaraque, L.G., Benítez-Páez,
506 A., Sarabi-Jamab, M., Ghorani, B., & Lopez-Rubio, A. (2019). Agarose-based freeze-dried
507 capsules prepared by the oil-induced biphasic hydrogel particle formation approach for the
508 protection of sensitive probiotic bacteria. *Food Hydrocolloids*, 87, 487-496.

509 Ansari, S. A., & Husain, Q. (2012). Potential applications of enzymes immobilized on/in nano
510 materials: A review. *Biotechnology Advances*, 30(3), 512–523.

511 Aymard, P., Martin, D.R., Plucknett, K., Foster, T.J., Clark, A.H., & Norton, I.T. (2001).
512 Influence of thermal history on the structural and mechanical properties of agarose gels.
513 *Biopolymers*, 59 (3), 131–144.

514 Bilal, M., & Iqbal, H.M.N. (2019). Naturally-derived biopolymers: Potential platforms for
515 enzyme immobilization. *International Journal of Biological Macromolecules*, 130, 462-482.

516 Chen, W., Chen, H., Xia, Y., Zhao, J., Tian, F., & Zhang, H. (2008). Production, Purification,
517 and Characterization of a Potential Thermostable Galactosidase for Milk Lactose Hydrolysis from
518 *Bacillus stearothermophilus*. *Journal of Dairy Science*, 91(5), 1751–1758.

519 Chopin, T., Kerin, B. F., & Mazerolle, R. (1999). Phycocolloid chemistry as a taxonomic indicator
520 of phylogeny in the Gigartinales, Rhodophyceae: A review and current developments using
521 Fourier transform infrared diffuse reflectance spectroscopy. *Phycological Research*, 47(3), 167–
522 188

523 Chui, M., Philips, R., & McCarthy, M. (1995). Measurement of the porous microstructure of
524 hydrogels by nuclear magnetic resonance. *Journal of Colloid Interface Science*, 174, 336–344.

525 Cipolatti, E.P., Valério, A., Henriques, R.O., Moritz, D.E., Ninow, J.L., Freire, D.M.G., Manoel,
526 E.A., Fernandez-Lafuente, R., & De Oliveira, D. (2016). Nanomaterials for biocatalyst
527 immobilization-state of the art and future trends. *RSC Advances*, 6 (106), 104675-104692.

528 Comin, L.M., Temelli, F., & Saldaña, M.D.A. (2012). Barley beta-glucan aerogels via
529 supercritical CO₂ drying. *Food Research International*, 48, 442-448.

530 Cui, J., & Jia, S. (2017). Organic–inorganic hybrid nanoflowers: A novel host platform for
531 immobilizing biomolecules. *Coordination Chemistry Reviews*, 352(29), 249–263.

532 Dekker, P., J.T., Koenders, D. & Bruins, M (2019). Lactose-Free Dairy Products: Market
533 Developments, Production, Nutrition and Health Benefits. *Nutrients* 11, n.º 3 (5 de marzo de
534 2019): 551. <https://doi.org/10.3390/nu11030551>.

535 Drozdov, A.D., Papadimitriou, A.A., Liely, J.H.M, & Sanporean, C. G. (2016). Constitutive
536 equations for the kinetics of swelling of hydrogels. *Mechanics of Materials*, 102, 61-73.

537 Estevinho, B.N., Samaniego, N., Talens-Perales, D., Fabra, M.J., López-Rubio, A., Polaina, J., &
538 Marín-Navarro, J.(2018). Development of enzymatically-active bacterial cellulose membranes
539 through stable immobilization of an engineered β -galactosidase. *International Journal of*
540 *Biological Macromolecules*, 115, 476-482.

541 Fabra, M.J., Pérez-Bassart, Z., Talens-Perales, D., Martínez-Sanz, M., López-Rubio, A., Marín-
542 Navarro, J., & Polaina, J. (2019). Matryoshka enzyme encapsulation: Development of zymoactive
543 hydrogel particles with efficient lactose hydrolysis capability. *Food Hydrocolloids*, 96, 171-177

544 Faraj, A., Lebbar, T., Debry, G., & Najim, L. (1987). Protein and amino acids analysis during
545 alimentary-agar extraction from *Gelidium sesquipedale*, *Hydrobiologia*, 151 (1), 513–522.

546 Ge, J., Lei, J., & Zare, R. N. (2012). Protein–inorganic hybrid nanoflowers. *Nature*
547 *nanotechnology*, 7(7), 428-432.

548 Gómez-Ordóñez, E., & Rupérez, P. (2011). FTIR-ATR spectroscopy as a tool for polysaccharide
549 identification in edible brown and red seaweeds, *Food Hydrocolloids*, 25 (6), 1514–1520.

550 Grosová, Z., Rosenberg, M., & Rebroš, M. (2008). Perspectives and applications of immobilized
551 β -galactosidase in food industry - A review. *Czech Journal of Food Sciences*, 26(1), 1–14.

552 Guenet, J.-M., & Rochas, C. (2006). Agarose sols and gels revisited. *Macromolecular*
553 *Symposium*, 242, 65–70.

554 Hasanzadeh, M., Shadjou, N., & de la Guardia, M. (2018). Nanosized hydrophobic gels:
555 Advanced supramolecules for use in electrochemical bio- and immunosensing. *TrAC - Trends in*
556 *Analytical Chemistry*, 102, 210-224.

557 Hong, T., Liu, W., Li, M., & Chen, C. (2019). Recent advances in the fabrication and application
558 of nanomaterial-based enzymatic microsystems in chemical and biological sciences. *Analytica*
559 *Chimica Acta*, 1067, 31-47.

560 Huber, R., Langworthy, T. A., Knig, H., Thomm, M., Woese, C. R., Sleytr, U. B., & Stetter, K.
561 O. (1986). *Thermotoga maritima* sp. nov. represents a new genus of unique extremely
562 thermophilic eubacteria growing up to 90o C. *Archives of Microbiology*, 144, 324–325.

563 Kim, C. S., Ji, E. S., & Oh, D. K. (2004). Characterization of a thermostable recombinant β -
564 galactosidase from *Thermotoga maritima*. *Journal of Applied Microbiology*, 97(5), 1006–1014

565 Lai, M.-F., & Lii, C.-Y. (1997). Rheological and thermal characteristics of gel structures from
566 various agar fractions. *International Journal of Biological Macromolecules*, 21 (1), 123–130.

567 Labropoulos, K.C., Niesz, D.E., Danforth, S.C., & Kevrekidis, P.G. (2002). Dynamic rheology
568 of agar gels: theory and experiments. Part I. Development of a rheological model. *Carbohydrate*
569 *Polymers*, 50, 393–406.

570 Lee, W.-K., Lim, Y.-Y., Leow, A.T.-C., Namasivayam, P., Abdullah, J.O., & Ho, C.-L. (2017).
571 Factors affecting yield and gelling properties of agar. *Journal of Applied Phycology*, 29 (3), 1527–
572 1540.

573 Levy-Ontman, O., Blum, D., Golden, R., Pierschel, E., Leviev, S., & Wolfson, A. (2019).
574 Palladium Based-Polysaccharide Hydrogels as Catalysts in the Suzuki Cross-Coupling Reaction.

575 *Journal of Inorganic and Organometallic Polymers and Materials*, DOI: 10.1007/s10904-019-
576 01221-0

577 Liese, A., & Hilterhaus, L. (2013). Evaluation of immobilized enzymes for industrial applications.
578 *Chemical Society Reviews*, 42(15), 6236–6249.

579 Liu, Y., Ji, X., & He, Z. (2019). Organic-inorganic nanoflowers: from design strategy to
580 biomedical
581 applications. *Nanoscale*, 11, 17179.

582 Manzocco, L., Valoppi, F., Calligaris, S., Andreatta, F., Spilimbergo, S., & Nicoli, M.C. (2017).
583 Exploitation of κ -carrageenan aerogels as template for edible oleogel preparation. *Food*
584 *Hydrocolloids*, 71, 68-75.

585 Marín-Navarro, J., Talens-Perales, D., Oude-Vrielink, A., Cañada, F.J., & Polaina, J. (2014).
586 Immobilization of thermostable β -galactosidase on epoxy support and its use for lactose
587 hydrolysis and galactooligosaccharides biosynthesis. *World Journal of Microbiology and*
588 *Biotechnology*, 30 (3), 989-998.

589 Martínez-Sanz, M., Gómez-Mascaraque, L.G., Ballester, A.R., Martínez-Abad, A., Brodkorb, A.,
590 & López-Rubio, A. (2019). Production of unpurified agar-based extracts from red seaweed
591 *Gelidium sesquipedale* by means of simplified extraction protocols. *Algal Research*, 38, art. no.
592 101420.

593 Mattar, R., Ferraz De Campos, D., Flair, M., & Carrilho, J. (2012). Clinical and Experimental
594 Gastroenterology Lactose intolerance: diagnosis, genetic, and clinical factors. *Clinical and*
595 *Experimental Gastroenterology*, 5, 113–121.

596 Matsuo, M., Tanaka, T., & Ma, L. (2002). Gelation mechanism of agarose and κ -carrageenan
597 solutions estimated in terms of concentration fluctuation. *Polymer*, 43, 5299–5309.

598 Míguez-Amil, S., Jimenez-Ortega, E., Ramirez, M., Talens-Perales, D., Marín-Navarro, J.,
599 Polaina, J., Sanz-Aparicio, J., & Fernández-Leiro, R. (2020). The cryo-EM structure of

600 *Thermotoga maritima* β -galactosidase: quaternary structure guides protein engineering. *ACS*
601 *Chemical Biology*, 15 179-188

602 Nieto, M., Nardecchia, S., Peinado, C., Catalina, F., Abrusci, C., Gutiérrez, M.C., Ferrer, M.L.,
603 & del Monte, F. (2010). Enzyme-induced graft polymerization for preparation of hydrogels:
604 synergetic effect of laccase-immobilized-cryogels for pollutants adsorption. *Soft Matter*, 6
605 (2010), p. 3533

606 Nordqvist, D., & Vilgis, T. (2011). Rheological study of the gelation process of agarose-based
607 solutions. *Food Biophysics*, 6, 450–460.

608 Nweke, M. C., Turmaine, M., McCartney, R. G., & Bracewell, D. G. (2017). Drying techniques
609 for the visualisation of agarose-based chromatography media by scanning electron microscopy.
610 *Biotechnology Journal*, 12(3).

611 Panesar, P. S., Kumari, S., & Panesar, R. (2010). Potential Applications of Immobilized β -
612 Galactosidase in Food Processing Industries. *Enzyme Research*, 2010, 1–16

613 Plou, F. J., Polaina, J., Sanz-Aparicio, J., & Fernández-Lobato, M. (2017). β -Galactosidases for
614 Lactose Hydrolysis and Galactooligosaccharide Synthesis. En C. Ray, R. and M. Rosell, C. (Eds.).
615 *Microbial Enzyme Technology in Food Applications* (pp. 121-144). CRC Press. Taylor and
616 Francis group.

617 Shankar, S., & Rhim, J. W. (2017). Preparation and characterization of agar/lignin/silver
618 nanoparticles composite films with ultraviolet light barrier and antibacterial properties.
619 *Food Hydrocolloids*, 71, 76–84.

620 Silanikove, N., Leitner, G., & Merin, U. (2015). The interrelationships between lactose
621 intolerance and the modern dairy industry: global perspectives in evolutionary and historical
622 backgrounds. *Nutrients*, 7 (2015), 7312-7331.

623 Stanley, N. F. (2006). Agar. In: *Food Polysaccharides and their Application*, pp. 186–204.
624 Stephen, A. M., Philips, G. O., and Williams, P. A., Eds., CRC Press, Boca Raton, FL

625 Rhim, J. W., Wang, L. F., Lee, Y., & Hong, S. I. (2014). Preparation and characterization of bio-
626 nanocomposite films of agar and silver nanoparticles: Laser ablation method. *Carbohydrate*
627 *Polymers*, 103, 456–465.

628 Talens-Perales, D., Fabra, M.J., Martínez-Argente, L., Martín-Navarro, N., & Polaina, J. (2020).
629 Recyclable, thermostable hybrid protein-inorganic nanoflowers: an efficient tool for the
630 hydrolysis of milk lactose. *International Journal of Biological Macromolecules*, 151, 602-608.

631 Ubeyitogullari, A., Brahma, S., Rose, D.J., & Ciftci, O.N. (2018). In Vitro Digestibility of
632 Nanoporous Wheat Starch Aerogels. *Journal of Agricultural and Food Chemistry*, 66 (36), 9490-
633 9497.

634 Volery, P., Besson, R., & Schaffer-Lequart, C. (2004). Characterization of commercial
635 carrageenans by Fourier transform infrared spectroscopy using single-reflection attenuated total
636 reflection. *Journal of Agricultural and Food Chemistry*, 52(25), 7457–7463

637 Wang, M., Mohanty, S.K., & Mohanty, S. (2019). Nanomaterial-Supported Enzymes for Water
638 Purification and Monitoring in Point-of-Use Water Supply Systems. *Accounts of Chemical*
639 *Research*, 52 (4), 876-885.

640 Zhao, F., Wang, Q., Dong, J., Xian, M., Yu, J., Yin, H., & Wang, J. (2017). Enzyme-inorganic
641 nanoflowers/alginate microbeads: An enzyme immobilization system and its potential
642 application. *Process Biochemistry*, 57(December 2016), 87–94.

643 Zolnere, K., & Ciprovica, I. (2018). The comparison of commercially available β -galactosidases
644 for dairy industry : review. *Food Science*, 1, 215–222.

645
646
647
648
649
650

651 **Table 1.** Specific hydrolytic activity, measured at 30 min, of the free TmLac, TmLac-Ca²⁺ nanoflowers
652 (TmLac NF) and TmLac-Ca²⁺ nanoflowers encapsulated in commercial agar (AA), unpurified agar (u-
653 AA) and agarose (Ag). Mean value (standard deviation).

654

Material	Activity ($\mu\text{mol Glc} \cdot \text{min}^{-1} \cdot \text{mg}^{-1}$)
TmLac	23.8 \pm 1.0 ^a
TmLac NF	23.5 \pm 1.4 ^{ab}
AA	15.3 \pm 1.6 ^c
u-AA	17.2 \pm 2.6 ^{bc}
Ag	16.1 \pm 2.7 ^{bc}

655 Mean value \pm standard deviation

656 Different letters in superscripts (a-c) indicate significant differences ($p < 0.05$) among the samples.

657

658

659

660

661

662

663

664

665

666

667 **Table 2.** Gel strength of commercial agar (AA⁻), commercial agar with TmLac-Ca²⁺ nanoflowers
668 (AA), agarose (Ag⁻) and agarose with TmLac-Ca²⁺ nanoflowers (Ag) hydrogel capsules. Mean value
669 (standard deviation).

670

Material	F/d (N/mm)
AA -	0.37 ± 0.03 ^a
AA	0.41 ± 0.02 ^a
Ag -	0.42 ± 0.03 ^a
Ag	0.22 ± 0.02 ^b

671 Mean value ± standard deviation

672 Different letters in superscripts (a-b) indicate significant differences (p<0.05) among the samples

673

674

675

676

677

678

679

680

681

682

683

684

685

686 **Figure Captions**

687 **Figure 1** Visual appearance of hydrogel capsules with and without nanoflowers: (A) commercial agar,
688 (B) commercial agar with TmLac-Ca²⁺ nanoflowers, (C) unpurified agar, (D) unpurified agar with
689 TmLac-Ca²⁺ nanoflowers, (E) agarose and (F) agarose with TmLac-Ca²⁺ nanoflowers.

690 **Figure 2** Hydrolysis of lactose by free TmLac (TmLac), TmLac-Ca²⁺ nanoflowers (TmLac NF) and
691 enzymatically active hydrogel capsules made of either commercial agar (AA), unpurified agar (u-AA)
692 and agarose (Ag).

693 **Figure 3** Hydrolysis of lactose (5% solution) after serial batches of incubation, at 75 °C for 70 min, of
694 TmLac-Ca²⁺ nanoflowers and hydrogel capsules based on commercial agar (AA), unpurified agar (u-
695 AA) and agarose loaded with TmLac-Ca²⁺ nanoflowers.

696 **Figure 4** Visual appearance of aerogel capsules with and without nanoflowers: (A) commercial agar
697 with TmLac-Ca²⁺ nanoflowers, (B) unpurified agar with TmLac-Ca²⁺ nanoflowers and (C) agarose
698 with TmLac-Ca²⁺ nanoflowers.

699 **Figure 5** Representative SEM images of the aerogel capsules with and without nanoflowers: (A)
700 commercial agar, (B) unpurified agar and (C) agarose (scale markers are 1 mm and 5 µm for left and
701 right micrographs, respectively),

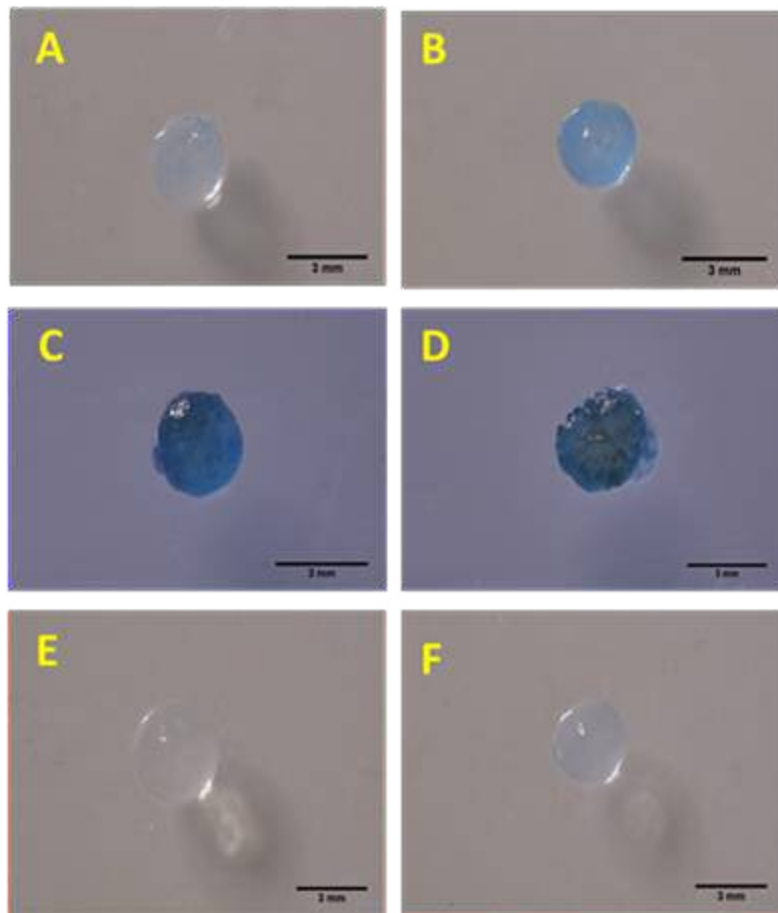
702 **Figure 6** Representative SEM micrographs and binary images of the porosity degree of aerogel
703 capsules with and without nanoflowers: (A) commercial agar, (B) unpurified agar and (C) agarose.
704 (scale marker 10 µm). The porosity area is given in percentage.

705 **Figure 7** ATR-FTIR spectra from loaded and unloaded aerogels based on commercial agar, unpurified
706 agar and agarose.

707 **Figure 8** Hydrolysis of lactose by freeze-dried TmLac (TmLac-FD), freeze-dried TmLac-Ca²⁺
708 nanoflowers (TmLac NF-FD) and enzymatically active aerogel capsules made of commercial agar
709 (AA-FD).

710 **Figure 9** Hydrolysis of lactose (5% solution) after serial batches of incubation, at 75 °C for 70 min
711 agar-based aerogels (AA-FD).

1 **Figure 1**



2

3

4

5

6

7

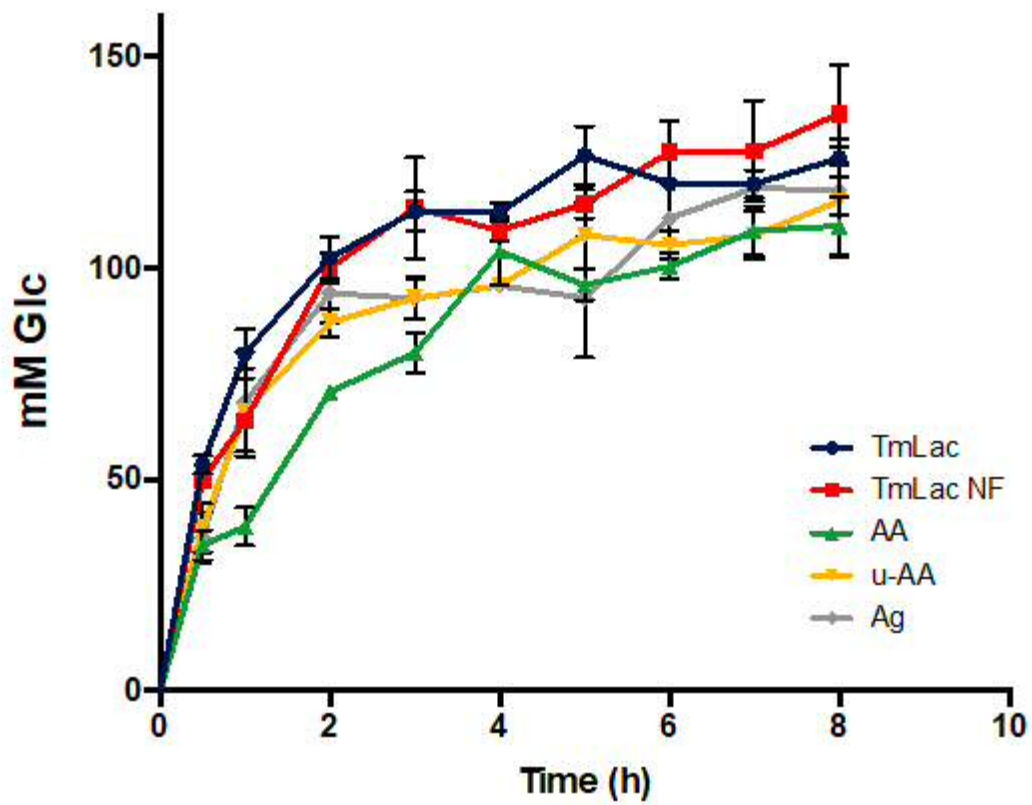
8

9

10

11

12 Figure 2.



13

14

15

16

17

18

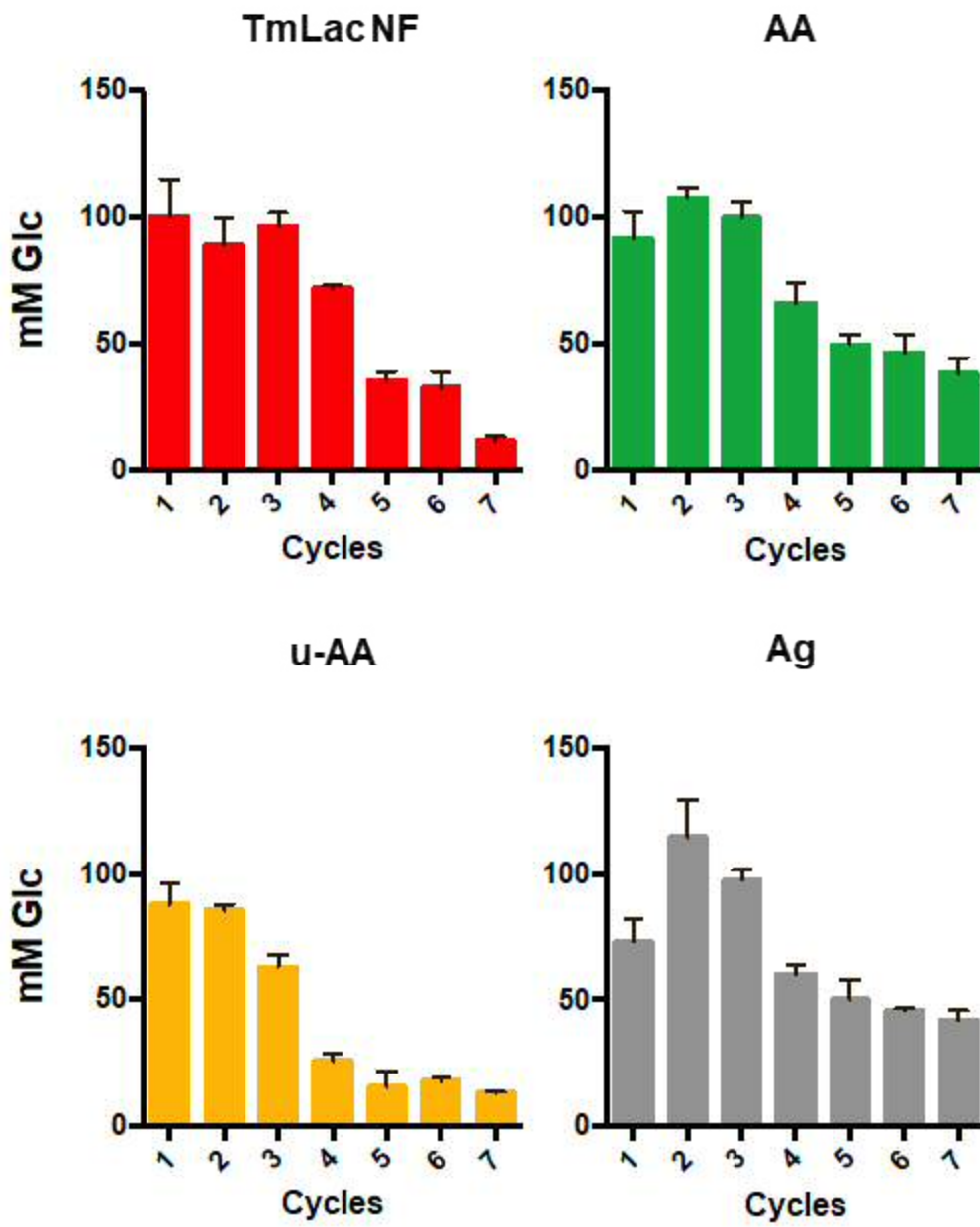
19

20

21

22

23 **Figure 3**



24

25

26

27

28

29

30 **Figure 4**

31



32

33

34

35

36

37

38

39

40

41

42

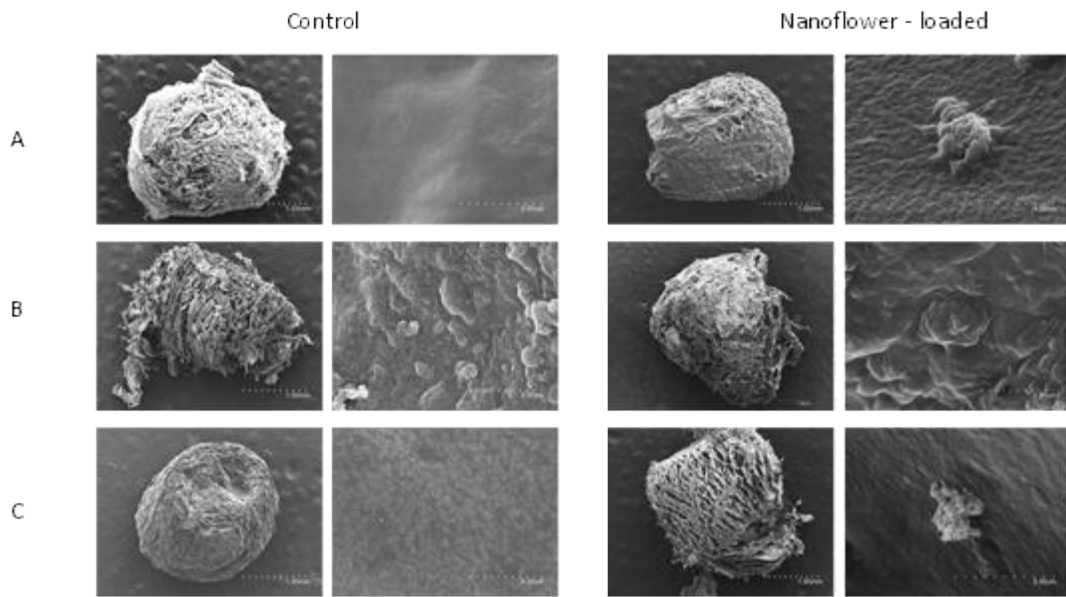
43

44

45

46

47 **Figure 5.**



48

49

50

51

52

53

54

55

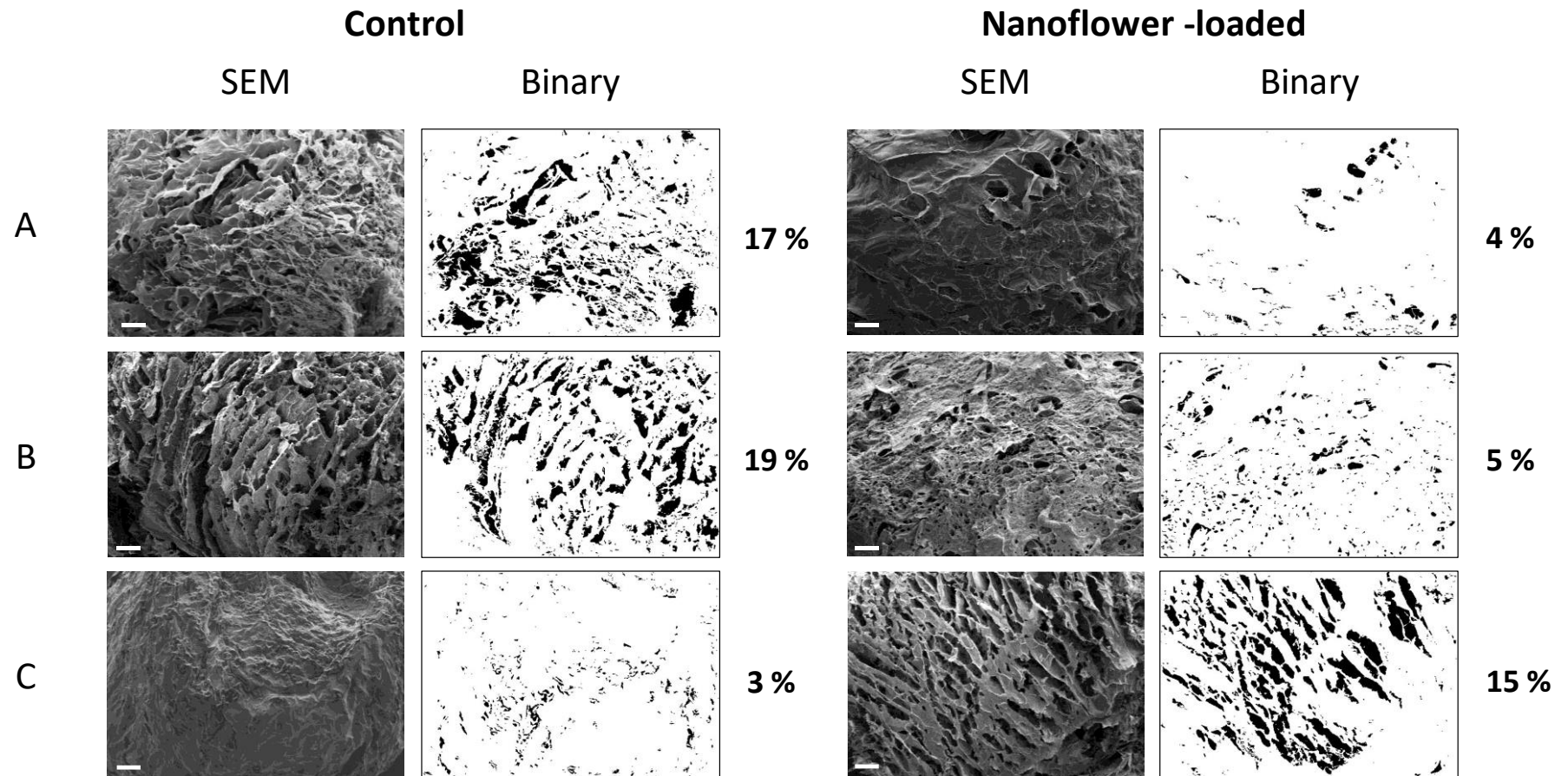
56

57

58

59

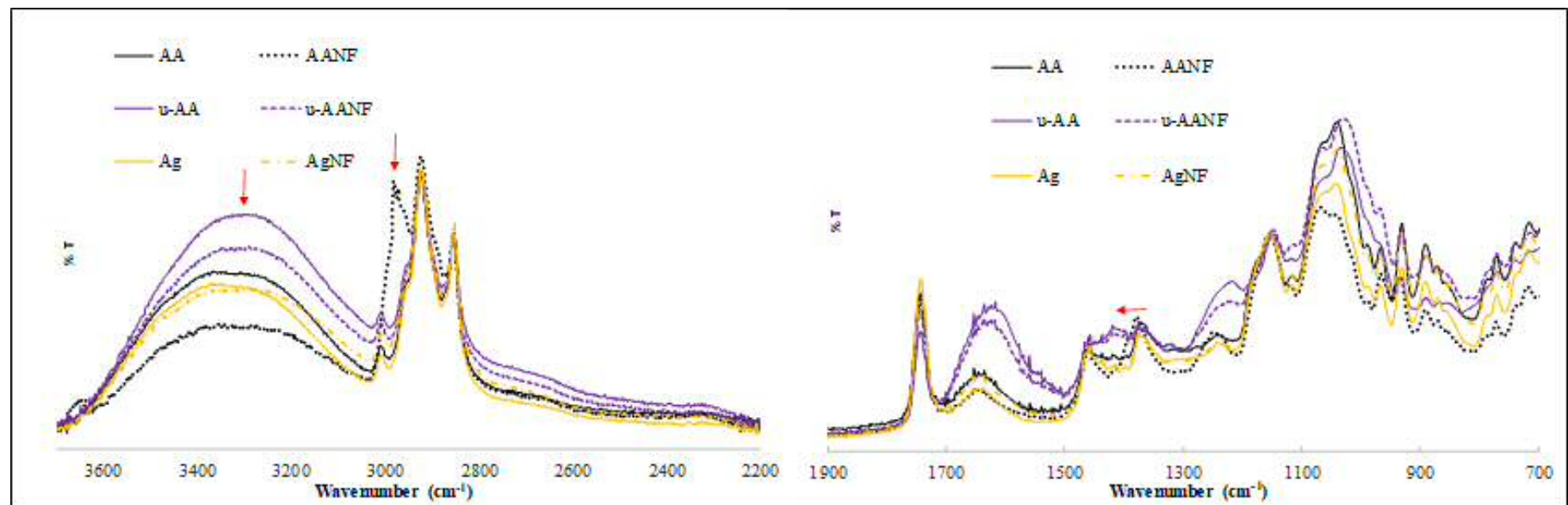
60 **Figure 6**



61

62

63 **Figure 7**



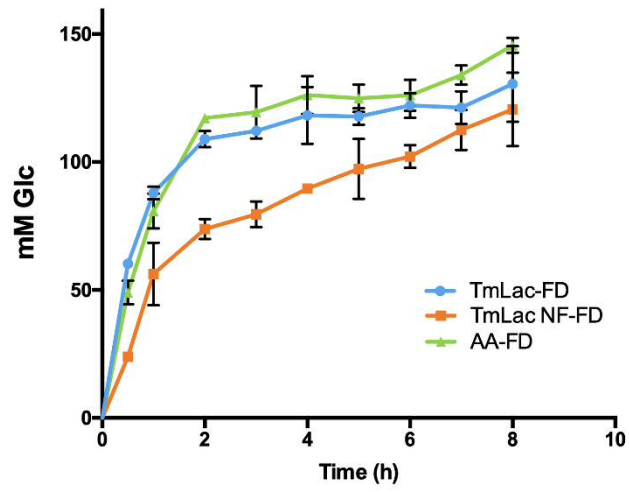
64

65

66

67

68 **Figure 8**



69

70

71

72

73

74

75

76

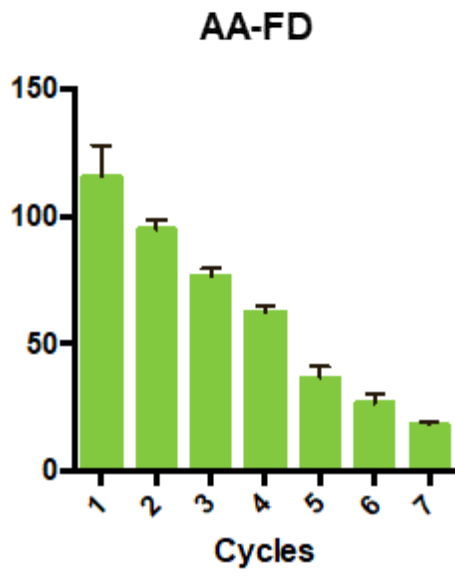
77

78

79

80

81 **Figure 9**



82

83

84

85

Highlights:

- TmLac-nanoflowers were encapsulated in marine polysaccharide hydrogels and aerogels
- Enzymatic activity was more efficiently preserved in purified agar hydrogels/aerogels
- Active aerogels based on commercial agar showed the highest catalytic activity
- 0.5 g of aerogel beads hydrolyze the lactose equivalent of 100 mL of milk in 15 min